JCI The Journal of Clinical Investigation

Impaired humoral and cellular immunity after SARS-CoV-2 BNT162b2 (tozinameran) prime-boost vaccination in kidney transplant recipients

Arne Sattler, Eva Schrezenmeier, Ulrike A. Weber, Alexander Potekhin, Friederike Bachmann, Henriette Straub-Hohenbleicher, Klemens Budde, Elena Storz, Vanessa Proß, Yasmin Bergmann, Linda M.L. Thole, Caroline Tizian, Oliver Hölsken, Andreas Diefenbach, Hubert Schrezenmeier, Bernd Jahrsdörfer, Tomasz Zemojtel, Katharina Jechow, Christian Conrad, Sören Lukassen, Diana Stauch, Nils Lachmann, Mira Choi, Fabian Halleck, Katja Kotsch

J Clin Invest. 2021;131(14):e150175. https://doi.org/10.1172/JCI150175.

Research Article **Immunology**

Graphical abstract

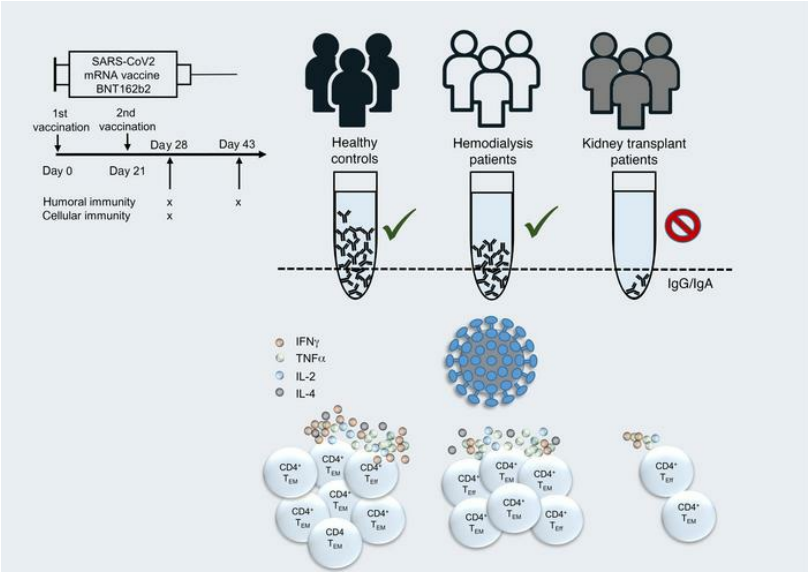

Impaired humoral and cellular immunity after SARS-CoV-2 BNT162b2 (tozinameran) prime-boost vaccination in kidney transplant recipients

Arne Sattler,[1] Eva Schrezenmeier,[2] Ulrike A. Weber,[2] Alexander Potekhin,[2,3] Friederike Bachmann,[2] Henriette Straub-Hohenbleicher,[2] Klemens Budde,[2] Elena Storz,[1] Vanessa Proß,[1] Yasmin Bergmann,[1] Linda M.L. Thole,[1] Caroline Tizian,[4] Oliver Hölsken,[4,5] Andreas Diefenbach,[4] Hubert Schrezenmeier,[6] Bernd Jahrsdörfer,[6] Tomasz Zemojtel,[7] Katharina Jechow,[8] Christian Conrad,[8] Sören Lukassen,[8] Diana Stauch,[9] Nils Lachmann,[9] Mira Choi,[2] Fabian Halleck,[2] and Katja Kotsch[1]

[1]Department for General and Visceral Surgery and [2]Department of Nephrology and Intensive Care, Charité–Universitätsmedizin Berlin, corporate member of Freie Universität Berlin, Humboldt-Universität zu Berlin, and Berlin Institute of Health (BIH), Berlin, Germany. [3]MVZ Diaverum Neubrandenburg, Neubrandenburg, Germany. [4]Laboratory of Innate Immunity, Department of Microbiology, Infectious Diseases and Immunology, Charité–Universitätsmedizin Berlin, corporate member of Freie Universität Berlin, Humboldt-Universität zu Berlin, and BIH, Berlin, Germany. [5]Heidelberg Bioscience International Graduate School, Heidelberg University, Heidelberg, Germany. [6]Department of Transfusion Medicine and Institute for Clinical Transfusion Medicine and Immunogenetics, German Red Cross Blood Transfusion Service, Baden-Württemberg—Hessen and University Hospital Ulm, Ulm University, Ulm, Germany. [7]Genomics Core Facility, [8]Center for Digital Health, and [9]HLA Laboratory, Charité–Universitätsmedizin Berlin, corporate member of Freie Universität Berlin, Humboldt-Universität zu Berlin, and BIH, Berlin, Germany.

Novel mRNA-based vaccines have been proven to be powerful tools in combating the global pandemic caused by SARS-CoV-2, with BNT162b2 (trade name: Comirnaty) efficiently protecting individuals from COVID-19 across a broad age range. Still, it remains largely unknown how renal insufficiency and immunosuppressive medication affect development of vaccine-induced immunity. We therefore comprehensively analyzed humoral and cellular responses in kidney transplant recipients after the standard second vaccination dose. As opposed to all healthy vaccinees and the majority of hemodialysis patients, only 4 of 39 and 1 of 39 transplanted individuals showed IgA and IgG seroconversion at day 8 ± 1 after booster immunization, with minor changes until day 23 ± 5, respectively. Although most transplanted patients mounted spike-specific T helper cell responses, frequencies were significantly reduced compared with those in controls and dialysis patients and this was accompanied by a broad impairment in effector cytokine production, memory differentiation, and activation-related signatures. Spike-specific $CD8^+$ T cell responses were less abundant than their $CD4^+$ counterparts in healthy controls and hemodialysis patients and almost undetectable in transplant patients. Promotion of anti-HLA antibodies or acute rejection was not detected after vaccination. In summary, our data strongly suggest revised vaccination approaches in immunosuppressed patients, including individual immune monitoring for protection of this vulnerable group at risk of developing severe COVID-19.

Introduction

Kidney transplant (KTx) recipients and patients suffering from kidney failure are imperiled by increased infection risks, either due to dialysis-associated (reviewed in ref. 1) or therapeutic immunosuppression (IS). This has been comprehensively documented, e.g., for CMV, EBV, and BK virus infection (2), commonly affecting renal transplant recipients with potential implications for allograft function. A growing body of evidence indicates that both patient groups show considerably increased mortality after SARS-CoV-2 infection (3–6), arguing in favor of their prioritization in COVID-19 vaccination programs. Large-scale phase III clinical trials (7, 8) have meanwhile demonstrated impressive efficacy of novel mRNA-based vaccines in the prevention of severe illness or death. With respect to the BNT162b2 vaccine, humoral and cellular responses are documented to be efficiently triggered within 1 week after boost, with concomitant induction of specific helper and cytotoxic T cell responses (9). Recent data from a BNT162b2 mass vaccination campaign suggest slightly lower effectiveness in patients with comorbidities (10); however, no individual data sets are available for kidney diseases, and patients under immunosuppressive therapy were largely excluded from controlled trials. Therefore, accounting for all SARS-CoV-2 vaccines authorized thus far, information on kinetics and quality of specific immunity in KTx and hemodialysis (HD) patients remains scarce. Experience from influenza A/H1N1 (11, 12) and hepatitis B vaccination trials (13, 14) indicates lower humoral responder rates in both patient groups, likely resulting from combined impairment of early memory B and T cell formation (15). To provide pioneering data on mRNA vaccine–specific adaptive immunity, we quantified humoral and cellular responses induced by BNT162b2 in healthy controls (HCs) as compared with patients on HD and KTx recipients.

▶ **Related Commentary: https://doi.org/10.1172/JCI151178**

Authorship note: MC, FH, and KK are co–senior authors.
Conflict of interest: The authors have declared that no conflict of interest exists.

Submitted: April 1, 2021; **Accepted:** June 3, 2021; **Published:** July 15, 2021.
Reference information: *J Clin Invest*. 2021;131(14):e150175.
https://doi.org/10.1172/JCI150175.

In the latter group, SARS-CoV-2 spike–specific IgG and IgA were rarely detectable and were accompanied by broad quantitative and functional impairment of T cell responses. Our study highlights an urgent need for identifying alternative or modified immunization strategies for protection of these immunocompromised patients at high risk for SARS-CoV-2–associated morbidity and mortality.

Results

Study subjects. The study cohort consisted of 39 HCs (the majority of whom were health care professionals with high vaccination priority), 39 age-matched KTx recipients treated with standard immunosuppressive medication, and 26 individuals with kidney failure on HD. Details of their characteristics are summarized in Table 1. Because of current vaccination prioritization in Germany, subjects in the HD group exhibited a significantly higher mean age than HCs. The HD group was further characterized by higher proportions of patients with coronary heart disease and a history of liver disease as compared with transplanted individuals. All individuals were vaccinated with BNT162b2 (tozinameran) in January or February 2021 with a booster immunization after 21 days. Blood samples for cellular analysis were collected on day 8 ± 1 after boost. Specimens for assessment of humoral immunity were collected for all groups on day 0 and day 8 ± 1 after boost. Sera of 24 KTx patients were additionally analyzed on day 23 ± 5 after boost. Previous SARS-CoV-2 infection was excluded for all study subjects based on PCR test results, medical history, absence of serum reactivity in a SARS-CoV-2 nucleocapsid protein ELISA (pre and post vaccination) and/or spike protein–specific ELISA (pre vaccination). No de novo induction or increase of existing anti-HLA antibodies was detected in KTx patients at day 8 ± 1 after vaccination as compared with baseline, nor were signs of acute rejection recorded.

Absence of vaccination-induced humoral immunity in KTx patients. Humoral responses to BNT162b2 vaccination were determined by ELISA. Spike S1 domain–specific IgG reactivity was noted in all 39 HCs and 22 of 26 (84.62%) HD patients, but only in 1 of 39 (2.6%) KTx patients at day 8 ± 1 after boost. Comparisons of both patient groups with HCs showed significance. Similar findings were made with respect to IgA responses, where only 4 of 39 (10.26%) transplant recipients were seroreactive as compared with 38 of 39 (97.44%) HCs and 22 of 26 (84.62%) HD patients. Neutralizing antibodies were detected in all 39 HCs and 20 of 26 (76.92%) HD patients, but in none of the KTx patients examined; comparisons of both patient groups with HCs were again highly significant, respectively (Figure 1A). To decipher whether seroconversion kinetics for transplanted patients were delayed, samples available from 24 previous humoral nonresponders were reanalyzed at day 23 ± 5 after booster vaccination. At this time point, 2 of 24 (8.33%) patients showed IgG and 3 of 24 (13.04%) IgA seroconversion (Figure 1B). Relative quantification of spike-specific titers was conducted based on OD ratios. Accounting for both isotypes and neutralizing capacity, HCs exhibited significantly higher Ig levels than responding HD patients (Figure 1C); due to the low responder rate, statistical analysis for KTx patients was only performed with respect to IgA. Throughout, no signs of acute rejection were observed in KTx patients in response to vaccination during the observation period (day 0 to day 23 ± 5 after boost) or increased levels of HLA-specific antibodies recorded on day 8 ± 1 after booster immunization as compared with day 0 (Table 1).

Prevalence and magnitude of vaccine-specific T cell responses. For detection of SARS-CoV-2 spike glycoprotein or CMV/EBV/influenza control antigen-reactive T cells (CEF, overlapping peptide mixes containing both CD4 and CD8 epitopes, not to be confused with similarly named commercial products; for details, see Methods), PBMCs were stimulated with overlapping peptide pools, allowing activation of both $CD4^+$ and $CD8^+$ T cells in an HLA-type–independent manner (16). After pregating on live $CD3^+dump^-$ lymphocytes, antigen-reactive $CD4^+$ Th cells were identified based on coexpression of CD154 and CD137, as demonstrated earlier (17), allowing sensitive detection with low background (Supplemental Figure 1, A and C; supplemental material available online with this article; https://doi.org/10.1172/JCI150175DS1). A T cell response was considered positive when peptide mix–stimulated cultures contained at least 2-fold higher frequencies of $CD154^+CD137^+$ (for $CD4^+$ T cells) or $CD137^+IFN\text{-}\gamma^+$ (for $CD8^+$ T cells) cells as compared with the unstimulated control, with at least 20 events. In support of the response criteria, Supplemental Figure 1C depicts the highly significant increase of $CD4^+CD154^+CD137^+$ Th cells in spike-stimulated versus unstimulated samples from KTx patients, illustrating that stimulation indices (SI) were between 5 and 200 for all but 1 responding individual, who still met the lower cut-off of 2.

The overall prevalence of vaccinated individuals displaying spike-specific $CD4^+$ T cell responses was similar for HCs, KTx recipients, and dialysis patients, ranging from 92% to 100%, thereby equaling responder rates to CEF stimulation (Figure 2A). With respect to the magnitude of the response, however, KTx, but not HD, patients exhibited significantly reduced frequencies of spike-specific $CD154^+CD137^+$ Th cells as compared with HCs. This observation did not apply to frequencies of CEF-specific Th cells in transplant recipients (Figure 2B). Of note, the few transplanted individuals mounting IgA and/or IgG responses until day 23 ± 5 after boost were characterized by significantly higher frequencies of vaccine-specific Th cells than seronegative patients (Figure 2C).

BNT162b2-induced $CD8^+$ T cells were identified based on activation-dependent coexpression of CD137 and $IFN\text{-}\gamma^+$ (Supplemental Figure 1A). The combination of CD137 and IFN-γ was chosen due to its superior signal (stimulated) to noise (unstimulated) ratio as compared with single ($CD137^+$) or combined activation marker ($CD137^+CD69^+$) usage for identification of specific $CD8^+$ T cells (data not shown). Overall, the prevalence of spike-specific CD8 responses was lower than that determined for $CD4^+$ Th cells, with less than 50% responders within HCs and HD patients. Interestingly, vaccine-specific $CD8^+$ T cells were detectable only in 2 of 39 (5.13%) KTx patients, whereas no significant differences between groups were observed for CEF-specific $CD8^+$ T cells (Figure 2D). Frequencies of $CD8^+$ T cells in responders to spike stimulation did not significantly differ between HCs and HD patients; due to the limited number of responding KTx patients, frequencies were not tested for significant differences from those of HCs. Of note, frequencies of CEF-reactive $CD8^+$ T cells did not significantly differ between groups (Figure 2E).

Functional repertoire of BNT162b2-reactive T helper cells. Unsupervised analysis using t-distributed stochastic neighbor embedding (tSNE) of concatenated data sets from all responding patients

Table 1. Characteristics of HCs, KTx recipients, and HD patients enrolled.

Variable	HC (*n* = 39)	KTx (*n* = 39)	HD (*n* = 26)	*P* values
Age (mean yr ± SD)	53.03 (17.58)	57.38 (14.04)	67.39 (11.88)	0.2730/**0.0012**[A]
Females/males (%)	19 (48.72)/20 (51.28)	11 (28.21)/28 (71.79)	9 (34.62)/17 (65.38)	0.1026/0.3112[A]
White (%)	39 (100)	39 (100)	26 (100)	0.9999/0.9999[A]
Clinical parameters				
Time on dialysis (mean yr ± SD)			6.87 (5.07)	
Time since Tx (mean yr ± SD)		8.15 (6.09)		
Retransplantation (%)		6 (15.38)		
Acute graft rejection (%)[B]		0 (0)		
Promotion of HLA antibodies (%)[C]		0 (0)		
IS medication				
CS+Tac+MMF (%)		22 (56.41)		
CS+CyA+MMF (%)		13 (33.33)		
$mTOR_i$+MMF ± CS (%)		3 (7.69)		
$mTOR_i$+CyA+MMF (%)		1 (2.56)		
CMV seropositive pre-Tx (%)		26 (66.67)		
Comorbidities				
Hypertension (%)		37 (94.87)	22 (84.61)	0.2075[D]
Coronary heart disease (%)		11 (28.21)	15 (57.70)	**0.0220**[D]
History of myocardial infarction (%)		4 (10.26)	4 (15.38)	0.7034[D]
Diabetes (%)		12 (30.77)	12 (46.15)	0.2945[D]
History of liver disease (%)		4 (10.26)	9 (34.62)	**0.0257**[D]
COPD (%)		0 (0)	3 (11.54)	0.0595[D]
History of malignancy (%)		6 (15.38)	3 (11.54)	0.7307[D]

CS, corticosteroids; Tac, tacrolimus; CyA, cyclosporin A; $mTOR_i$, mTOR inhibitor; Tx, transplantation. [A]Comparison of HC vs. KTx/HC vs. HD. [B]During observation period (day 0 to day 23 ± 5 after boost). [C]Day 8 ± 1 after boost compared with baseline (day 0). [D]Comparison of KTx vs. HD. Bold text indicates statistically significant differences (Fisher's exact test).

per group pointed to a reduced production of effector cytokines following spike stimulation in KTx patients as compared with HCs and HD patients (Figure 3A). This finding was reproducible after manual gating, revealing significantly diminished portions of IFN-γ–, TNF-α–, and IL-2– as well as IL-4–secreting cells in transplanted individuals, whereas only portions of IFN-γ–secreting cells were diminished in HD patients. Interestingly, frequencies of CEF-activated Th cells from KTx patients were significantly reduced only regarding their IL-2 production capacity (Figure 3, B–E). The ability to coproduce more than 1 cytokine at a time was then investigated for IFN-γ, TNF-α, and IL-2, with IL-4 being excluded since data were not available for all transplanted patients. KTx recipients harbored significantly lower frequencies of spike-specific IFN-γ^+TNF-α^+IL-2^+ (triple$^+$) polyfunctional Th cells, associated with an enrichment of cells that produced none of the 3 cytokines. This observation also applied to polyfunctionality of CEF-specific responses. Frequencies of spike or CEF-specific triple$^+$ T cells were not significantly reduced in HD patients as compared with HCs (Figure 3F).

Memory differentiation, ex vivo proliferation, and activation state of spike-specific T helper cells. To decipher whether the functional impairment of vaccine-specific Th cells in KTx patients was accompanied by changes in memory formation, subset distribution was analyzed according to expression of CD45RO and CD62L. Whereas the majority of spike-specific Th cells within healthy individuals showed a CD45RO$^+$CD62L$^-$ effector memory-like (TEM-like) phenotype, their portions were strongly reduced in KTx patients and were reduced to a lower, but equally significant, extent in HD patients. In both transplant and HD patients, TEM-formation impairment was paralleled by a significant increase of short-lived CD45RO$^-$CD62L$^-$ effector cells. The latter observation also accounted for CEF-specific Th cells in KTx, but not in HD, patients (Figure 4, A and B). Overall, spike-specific, as opposed to CEF-specific, Th cells showed elevated ex vivo proliferation, as reflected by Ki67 expression. Surprisingly, frequencies of Ki67$^+$ cells were slightly, but significantly, elevated in KTx patients as compared with HCs (Figure 4C). In line with their augmented ex vivo proliferation, spike- but not control antigen–specific Th cells characteristically upregulated the activation/exhaustion-associated molecule PD-1 with no marked differences between groups (Figure 4D). Most spike-specific Th cells expressed the coactivating molecule CD28; in line with data on its downregulation upon frequent encounters with persistent viruses such as CMV and a CMV-driven expansion of CD28^{null} T helper cells in the posttransplantation phase (18), transplant recipients harbored slightly, but significantly, reduced portions of CD28$^+$ CEF-specific Th cells (Figure 4E).

Transcriptome analysis of vaccine-specific Th cells from KTx patients reveals downregulation of pathways involved in immune activation and cytokine signaling. To collect additional information on differential activation signatures between groups, vaccine-specific CD4$^+$ T cells from 3 to 4 individuals per group were sorted to high purity, typically yielding 200 cells (Supplemental Figure 1B). Low-input bulk RNA-Seq analysis indicated 49 versus 10 highly differentially expressed (absolute $\log_2$ fold change ≥ 1, FDR < 0.05) genes in KTx versus dialysis patients compared with healthy probands, respectively. Transcripts, e.g., for IFN-γ, Th1 differentiation-associated IL-12 receptor β_2 chain or TRAF3IP2 involved in NF-κB signaling, were strongly downregulated in transplanted individuals; labeling was limited to genes deemed relevant due to their immune-related function and robustness of detection (Figure 5A). Pathway analysis further revealed overall downregulation of hallmarks associated with cellular activation, including cytokine signaling, inflammatory responses, allograft rejection, or glycolysis, whereas TGF-β signaling motifs were upregulated in spike-specific Th cells of transplant patients. Although several gene sets showed patterns in HD patients similar to those of HCs, the enrichment scores of the HD patients remained consistently lower (Figure 5B). An overview of up- or downregulated hallmarks is provided in Supplemental Figure 4 (KTx vs. HC) and Supplemental Figure 5 (HD vs. HC), respectively.

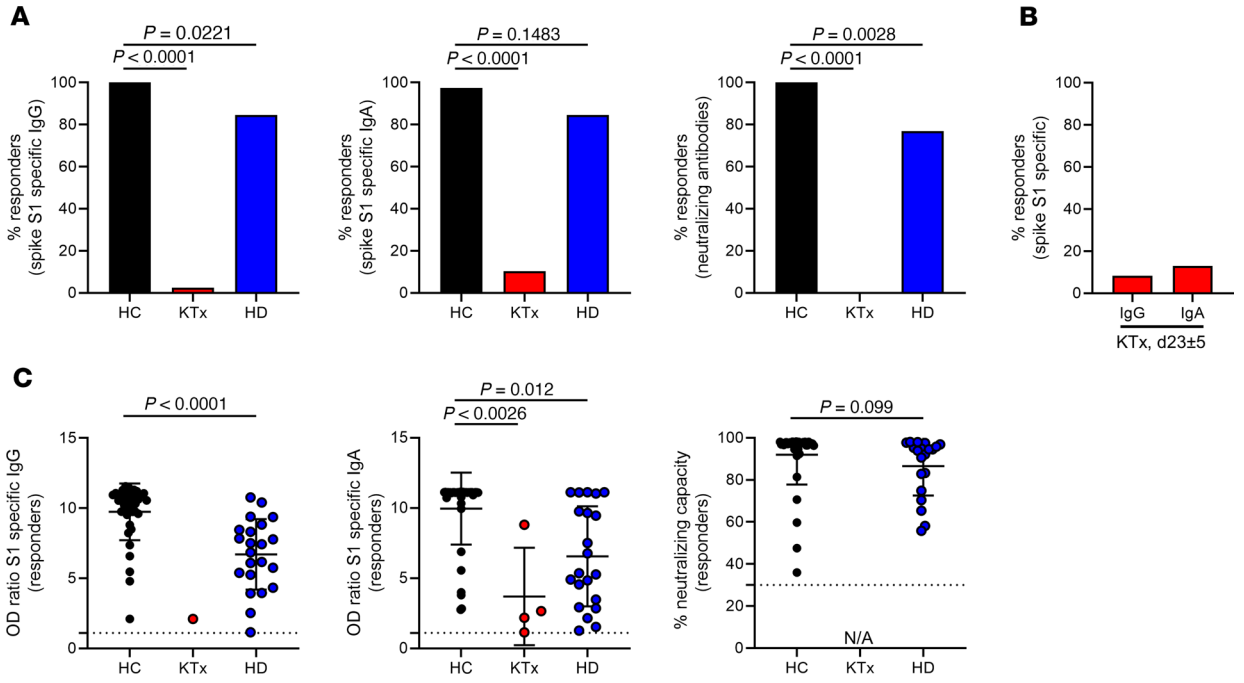

Figure 1. Humoral reactivity of vaccinees against SARS-CoV-2 spike protein. (**A**) Humoral responder rates were determined based on serum samples collected on day 8 ± 1 after boost being analyzed for spike S1 domain–specific IgG (left, Fisher's exact test) and IgA (middle, Fisher's exact test) by ELISA. Surrogate virus neutralization capacity was assessed by a blocking ELISA (right, Fisher's exact test) with HC (n = 39), KTx (n = 39), and HD (n = 26). (**B**) Sera of KTx patients available from day 23 ± 5 after boost immunization were retested for reactivity as in **A** with n = 24. (**C**) Serological reactivity was quantified only in responding individuals on day 8 ± 1 after boost. IgG, Mann-Whitney U test: HC, n = 39; KTx, n = 1; HD, n = 22. IgA, Kruskal-Wallis test: HC, n = 38; KTx, n = 0; HD, n = 21. Neutralization, Mann-Whitney U test: HC, n = 39; KTx, n = 0; HD, n = 20). NA, not applicable due to nonresponsiveness. Graphs show mean ± SD.

Impact of age and immunosuppressive medication on BNT162b2-induced cellular immunity. Individual predisposition, including age, might strongly affect antiviral immunity, as we have recently demonstrated for COVID-19 patients (17). To identify factors that might quantitatively shape vaccine-specific immunity, overall frequencies of $CD154^+CD137^+CD4^+$ T cells as well as the ex vivo proliferating $Ki67^+$ portion were therefore correlated with age for HCs, KTx recipients, and HD patients. Frequencies of spike-specific T cells did not correlate with age for HCs or HD patients, but showed a trend toward decreased portions with age for KTx patients (P = 0.0568). Whereas age in the HC group was positively correlated with frequencies of proliferating $Ki67^+$ Th cells, such association was not noted for KTx recipients or HD patients (Supplemental Figure 2A). Furthermore, we did not identify associations between time since transplantation and frequencies of spike-specific Th cells or those expressing Ki67 (Supplemental Figure 2B). Since most KTx patients uniformly received triple immunosuppressive medication and therapy mainly differed based on the type of calcineurin inhibitors (CNIs), subgroup analysis was performed for individuals receiving tacrolimus or cyclosporine A. Throughout, overall frequencies, portions of cytokine$^+$, proliferating, or $CD45RO^-CD62L^-$ effector-type Th cells did not show significant alterations between groups (Supplemental Figure 2C) with similar findings after stratification for low (≤ 1 g/d) or high (2 g/d) dose mycophenolate mofetil (MMF) therapy (Supplemental Figure 2D). In line with the aforementioned, no significant differences were found between tacrolimus- and cyclosporin A–treated KTx patients regarding quantitative and qualitative features of CEF-specific Th cells (Supplemental Figure 3).

Discussion

Based on large phase III clinical trials (7) and access to health care institution recordings (10), tremendous data sets are available suggesting high efficacy of SARS-CoV-2 vaccine BNT162b2 in preventing severe or fatal COVID-19 even in individuals with comorbidities or advanced age. Particularly the latter aspect has fueled the hope that, as opposed to what occurs with, e.g., varicella or influenza vaccines (reviewed in ref. 19), individuals with otherwise blunted vaccination outcomes might benefit from mRNA-based constructs. In this study, by assessing anti–SARS-CoV-2 mRNA vaccine-specific immunity, we identify a broad impairment of humoral and cellular responses in KTx recipients under standard triple immunosuppressive therapy. Whereas BNT162b2 was shown to efficiently induce spike-specific IgG and virus neutralization titers by day 8 after boost in healthy individuals (9), being in line with our observations, only few transplant recipients seroconverted until day 8 ± 1 after revaccination, with minor changes until day 23 ± 5. HD patients more frequently developed spike-specific humoral responses, although at rates still below those of HCs. The latter aspect matches inferior vaccination outcomes in HD patients reported after hepatitis B (20) or influenza A/H1N1 (11) inoculation.

Recently, Boyarsky et al. presented humoral response data after the second CoV-2 vaccination dose from a large cohort of different solid organ–transplant recipients, encompassing individuals with diverse ethnic backgrounds and immunosuppressive regimens (21). Due to the research letter format, no detailed information on the type of mRNA vaccine and immunosuppressive treatment could be extracted for the group of KTx recipients in whom

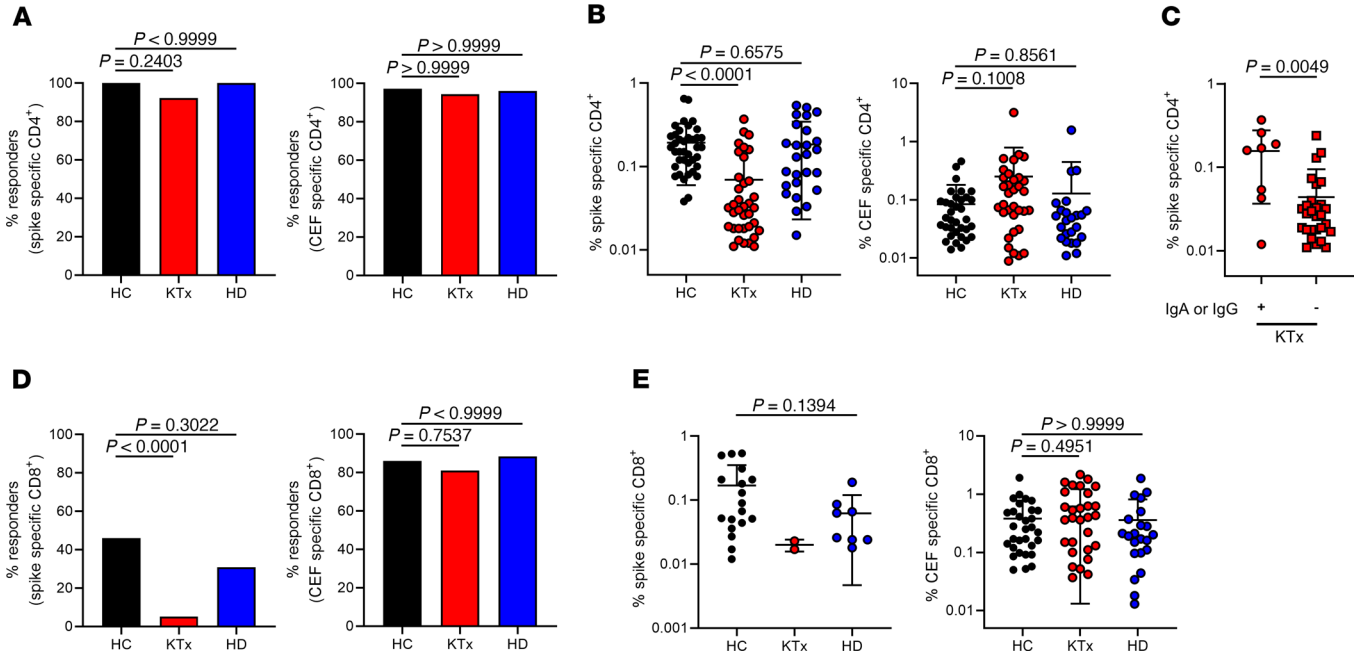

Figure 2. Quantitative features of spike-reactive T cells. (**A**) PBMCs were stimulated with spike (left) or CEF (right) peptide mix for 16 hours, as indicated. Specific CD4+ T cells were identified and quantified by FACS based on coexpression of CD154 and CD137. Depicted are percentages of HCs (n = 39), KTx recipients (n = 39), and HD patients (n = 26) with positive CD4+ T cell responses (responders: Fisher's exact test, respectively). (**B**) Frequencies of specific Th cells within responders. HC: spike, n = 39; CEF, n = 35; KTx: spike, n = 36; CEF, n = 34; HD: spike, n = 26; CEF, n = 24. Kruskal-Wallis test. (**C**) Portions of spike-specific Th cells in KTx patients showing IgA and/or IgG responses (+, n = 8) or not (–, n = 31; Mann-Whitney U test) until day 23 ± 5. (**D**) Antigen-specific CD8+ T cells were identified within PBMCs based on coexpression of CD137 and IFN-γ. Depicted are percentages within HCs (n = 39), KTx recipients (n = 39), and HD patients (n = 26) with positive CD8+ T cell responses (responders) toward spike (left, Fisher's exact test) or CEF (right, Fisher's exact test) stimulation. (**E**) Frequencies of spike-specific (left, Mann-Whitney U test) or CEF-specific CD8+ T cells (right, Kruskal-Wallis test) within responders. HC: spike, n = 18; CEF, n = 31; KTx: spike, n = 2. CEF, n = 30; HD: spike, n = 8; CEF, n = 22. Graphs show mean ± SD.

seroconversion was observed in 48% of individuals. Although not directly comparable to our data due to the aforementioned limitations, this study highlights antimetabolite therapy as critical for impairment of humoral responses, principally bearing the potential to directly affect B and plasma cell formation (22). The fact that all individuals in our cohort received MMF might provide an explanation for the comparably poor humoral responses observed. Similar effects might be attributable to glucocorticoids, as recently demonstrated for CoV-2–vaccinated patients with chronic inflammatory diseases (23), being a standard component of triple immunosuppressive medication in transplanted individuals.

Correlates of protection against COVID-19 are still incompletely understood and likely include immune components beyond neutralizing antibodies, with large animal models particularly highlighting the contribution of T cells upon viral rechallenge (24). Recent data from individuals with mild COVID-19 suggest a critical role for early induction of IFN-γ+ T cells, being associated with rapid viral clearance (25). With that background, our findings on broad quantitative and qualitative constraints of spike-specific Th cells in KTx patients raises the question of to what extent mRNA-based vaccination might confer protection in this vulnerable group. Using comprehensive multiparameter analysis, our data further reveal significant limitations of vaccine-specific Th effector functions in these individuals, applying to all cytokines examined and equally affecting polyfunctionality. T cells secreting multiple effector molecules at a time have gained particular attention due to their association with superior viral control in HIV-infected subjects (26), which was further verified for influenza infection (27). In context with vaccination, multipotent Th cells have been correlated with vaccine-induced immunity against tuberculosis (28). The presence of virus-reactive, multipotent T cells in convalescent seronegative individuals suggests a comparable role in protection against SARS-CoV-2 (29), with possible implications for its absence in KTx patients.

Interestingly, we found a significant correlation of age with frequencies of spike-specific Ki67+ T cells in HCs, but not in patients. A similar phenomenon has been documented for seasonal influenza vaccine–induced γ/δ T cells (30) and was speculated to be related to inflamm-aging (31), being characterized, e.g., by higher production of proproliferative cytokines such as IL-15 (32). The exact underlying driving forces, however, and their absence in KTx and HD patients, remain obscure and are beyond the scope of this study.

Extending flow cytometric data, low input transcriptome analysis of vaccine-specific T helper cells from transplant recipients highlighted downregulation of pathways involved in, e.g., cellular activation, cytokine signaling, and metabolism. Not surprisingly, these hallmarks represent footprints of immunosuppressive medication, as was shown for impaired IL-2/STAT5 signaling after kidney transplantation (33). Interestingly, IL-2 gene activity is also sensitive to TGF-β signaling (34), reflecting one of the features we found upregulated in Th cells from KTx patients. Among single genes, *TNF-SF4* (*OX40L*) showed increased transcript levels in this patient group; of note, OX40L protein upregulation was demonstrated only in Th cells after suboptimal

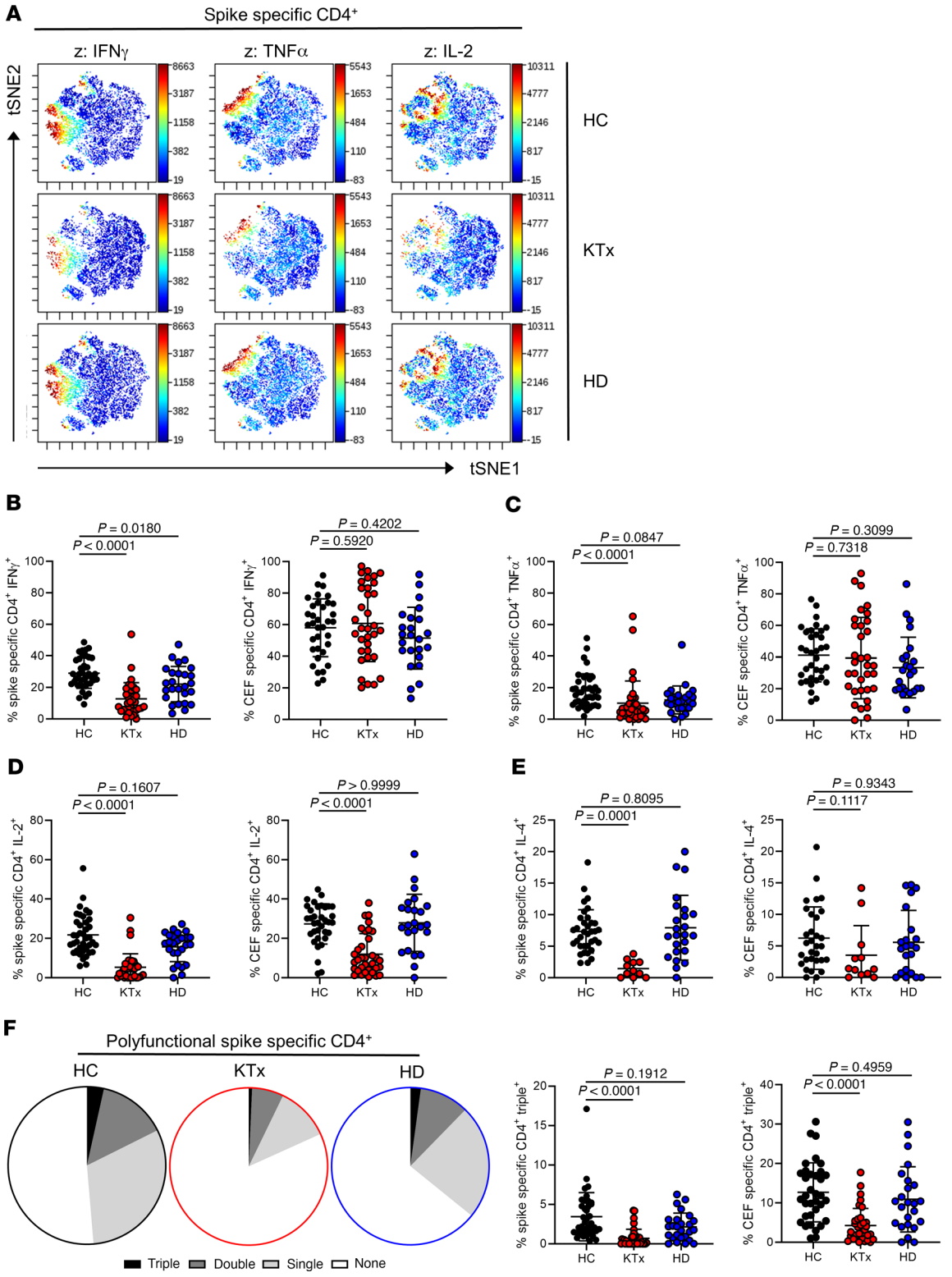

Figure 3. Functional assessment of vaccine-specific CD4⁺ Th cells. (**A**) Spike-specific CD154⁺CD137⁺ Th cells from all groups were concatenated and subjected to unsupervised analysis using tSNE; highlighted (*z* dimension) are areas with IFN-γ⁺, TNF-α⁺, or IL-2⁺ cells. Spike- or CEF-specific CD154⁺CD137⁺ Th cells were further examined after manual gating for expression of (**B**) IFN-γ (spike/CEF: ANOVA), (**C**) TNF-α (spike: Kruskal-Wallis test; CEF: ANOVA), (**D**) IL-2 (spike/CEF: Kruskal-Wallis test) with *n* as in Figure 2B, respectively, or (**E**) IL-4 (spike: ANOVA; CEF: Kruskal-Wallis test; HC: spike, *n* = 35; CEF: *n* = 31; KTx: spike, *n* = 11; CEF, *n* = 12; HD: spike, *n* = 24; CEF: *n* = 22). (**F**) Portions (left) of spike-specific T cells expressing 3, 2, 1, or 0 cytokines at a time based on the respective mean values of each group or (right) frequencies of spike- or CEF-specific Th cells staining triple positive for IFN-γ, TNF-α, and IL-2 with *n* as in Figure 2B and Kruskal-Wallis testing, respectively. IL-4 was excluded from polyfunctionality analyses due to the limited sample size in the KTx group. Graphs show mean ± SD.

antigenic stimulation (35) as is expected in immunosuppressed individuals. CNIs are further known to affect central components of T cell activation, such as NF-κB (36) and metabolic pathways, including glycolysis (37), both of which are mirrored in our pathway analyses.

Unexpectedly, we found quantity and quality of CEF-specific Th cells almost indistinguishable in immunosuppressed patients and HCs except for IL-2$^+$ and polyfunctional Th cells. Studies comparing recall responses to influenza infection versus vaccination in transplant recipients indicated that natural pathogen encounter entails much higher frequencies of antigen-specific T cells that consistently exhibited a broader functional repertoire (38), possibly resulting from strong innate costimulation. At least with respect to CMV and EBV, control antigen–specific responses in our KTx cohort relied on natural and most likely recurrent viral reactivation episodes, thereby providing a possible explanation for the enhanced cytokine production capacity toward CEF as compared with spike antigen stimulation. As a limitation, comprehensive documentation of viral infection, reactivation episodes, or vaccination was not available for our cohort, therefore not allowing us to assign CEF T cell reactivity to a particular pathogen.

Within vaccine-specific Th cells, KTx patients showed a distinct expansion of short-lived effector Th cells at the expense of the memory population. Impairment or retardation of memory formation might represent a direct effect of CNIs, as has been comparably demonstrated for Th1, Th2, and Th17 responses (39). Accounting both for functional repertoire and memory development, we cannot exclude different kinetics of vaccine-specific responses in patients as compared with HCs, since few KTx patients mounted humoral responses between day 8 and 23 after boost. Although they received higher vaccination dosage as compared with HCs, delayed mounting of specific T cell responses has been documented for HD patients after HBV vaccination, where both cytokine secretion capacity and memory formation normalized at later time points (20).

Whereas responder rates for CD4$^+$ Th cells were comparable between HCs and both patient groups in our study, spike-specific CD8$^+$ T cells were only detectable in 2 of 39 (5.13%) transplant recipients. Both vaccination and infection models have elegantly highlighted the importance of CD4 help for optimal development of memory CD8$^+$ T cell responses (40, 41), with CD4-derived IL-2 secretion being key for optimal CD8 priming and effector molecule synthesis (42). The fact that IL-2 production by spike-specific Th cells in KTx patients was strongly impaired, accompanied by downregulation of IL-2- and other cytokine signaling pathways, as suggested by RNA-Seq, may explain, in concert with direct effects of immunosuppressive therapy, the absence of vaccine-specific CD8$^+$ T cells in these individuals. Limitations of our study clearly include the small sample size and the homogeneity of the cohort with respect to ethnicity and immunosuppressive medication; furthermore, extension of the follow-up period will allow us to assess delayed seroconversion kinetics, as recently documented for dialysis patients (43).

In summary, we demonstrate here that despite advanced mean age and comorbidities, the majority of dialysis patients mounted humoral and cellular responses differing only in select features from healthy individuals. More importantly, however, our data have important implications for vaccination of immunosuppressed individuals, suggesting larger studies to address how different immunosuppressive regimens, vaccine type, dosage, and/or number of revaccinations might affect successful mounting of antiviral immunity. Based on the study by Boyarsky et al. (21), temporary tapering of antimetabolite therapy might be considered, provided that patients are closely monitored for graft function during such period. Further investigations are currently underway assessing the impact of additional booster doses that have been proven effective in the case of influenza A (H1N1) 2009 vaccination (44). Given the unexpectedly poor outcome of mRNA vaccine–induced responses in KTx patients, urgent action appears appropriate, affecting not only transplant recipients, but also individuals with other medical conditions requiring immunosuppressive therapy.

Methods

Study subjects and assessment of humoral immunity. Demographics of BNT162b2-vaccinated (tozinameran, BioNTech/Pfizer) healthy individuals and patients that had no history of PCR-confirmed SARS-CoV-2 infection are summarized in Table 1. Previous SARS-CoV-2 infection was further excluded by medical history in combination with a negative SARS-CoV-2 nucleoprotein–specific ELISA and/or a negative SARS-CoV-2 S1 IgG ELISA prevaccination (EUROIMMUN). Vaccine-specific humoral immunity was assessed in serum samples by ELISA-based analysis of SARS-CoV-2 spike S1 domain–specific IgG and IgA (EUROIMMUN). Samples were considered positive with OD ratios of greater than 1.1 as per the manufacturer's guidelines. An OD ratio value was determined by calculating the ratio of the OD of the respective test sample over the OD of the internal calibrator provided with the ELISA kit. For examination of virus-neutralization capacity, serum samples were analyzed using a surrogate SARS-CoV-2 neutralization test (sVNT, GenScript), as recently described (45). The blocking ELISA-based assay qualitatively detects anti–SARS-CoV-2 antibodies inhibiting the interaction between receptor-binding domain (RBD) of the viral spike glycoprotein and angiotensin-converting enzyme. According to the manufacturer′s protocol, inhibition scores of 30% or more were considered positive. HLA antibody screening was performed at baseline (day 0) and at day 8 ± 1 after boost. In a first broad Luminex screening approach, serum reactivity against a wide range of HLA class I and II antigens was tested (LABScreen Mixed Antigen Beads; One Lambda). In the case of a positive response, reactivity against single antigens was further tested (LABScreen Single Antigen Beads; One Lambda). Reactions exceeding a ratio of 1.5 in the LABScreen Mixed and a MFI value of 1000 in the single-antigen bead assay were considered positive. Promotion of anti-HLA antibodies was defined as any de novo induction or increase in reactions after vaccination compared with baseline. Tests were performed in a single run by the same technician to minimize interassay variability. Indications for acute graft rejection were based on changes in serum creatinine and/or albuminuria.

Antigens for cellular assays. Stimulations were performed with an overlapping peptide pool consisting of 15 mers with 11 amino acid overlap encompassing the full sequence of the SARS-CoV-2 (GenBank MN908947.3) spike glycoprotein (Pepmix, JPT). A combination of overlapping 15 mer peptide mixes including CMV (Peptivator pp65, Miltenyi Biotech), EBV (Peptivator Consensus, Miltenyi Biotech), and influenza H1N1 (Peptivator Matrix Protein 1 and Peptivator nucleoprotein, Miltenyi Biotech) served as control and is called CEF throughout. Antigens were used at a final concentration of 1 μg/ml per peptide.

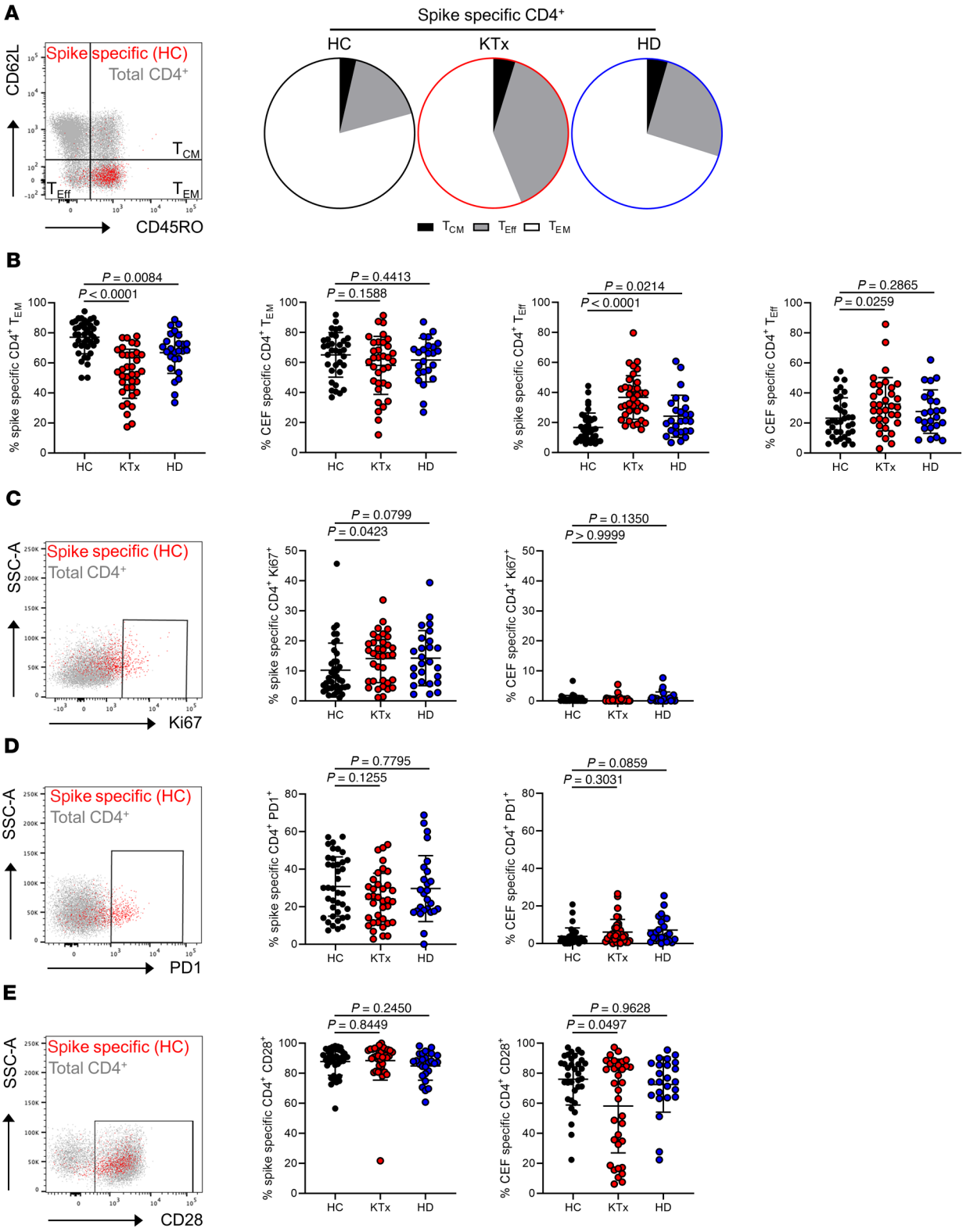

Figure 4. Characteristics of the spike-specific Th cell response with respect to memory formation and ex vivo proliferation/activation. Spike- or CEF-specific CD154$^+$CD137$^+$ Th cells were assessed for their memory or effector phenotype with CD45RO$^+$CD62L$^-$ identifying TEM, CD45RO$^+$CD62L$^+$ central memory (TCM), and CD45RO$^-$CD62L$^-$ effector-like T cells (TEff). (**A**) Exemplary staining of spike-specific vs. total Th cells from a healthy donor (left) and subset comparison based on the respective mean values for each group (right). (**B**) Data of spike- and CEF-specific TEM (left panels; spike/CEF: ANOVA) and TEff (right panels; spike/CEF: ANOVA) with *n* as in Figure 2B. Antigen-specific Th cells were further characterized for (**C**) ex vivo proliferation based on Ki67 expression (spike/CEF: Kruskal-Wallis test), (**D**) expression of the activation/exhaustion marker PD1 (spike: ANOVA, CEF: Kruskal-Wallis test), or (**E**) costimulatory receptor CD28 (spike/CEF: Kruskal-Wallis test) with exemplary overlays of spike-specific vs. total T cells (left) and summarized data for all groups (right) with *n* as in Figure 2B. SSC-A, side scatter area. Graphs show mean ± SD.

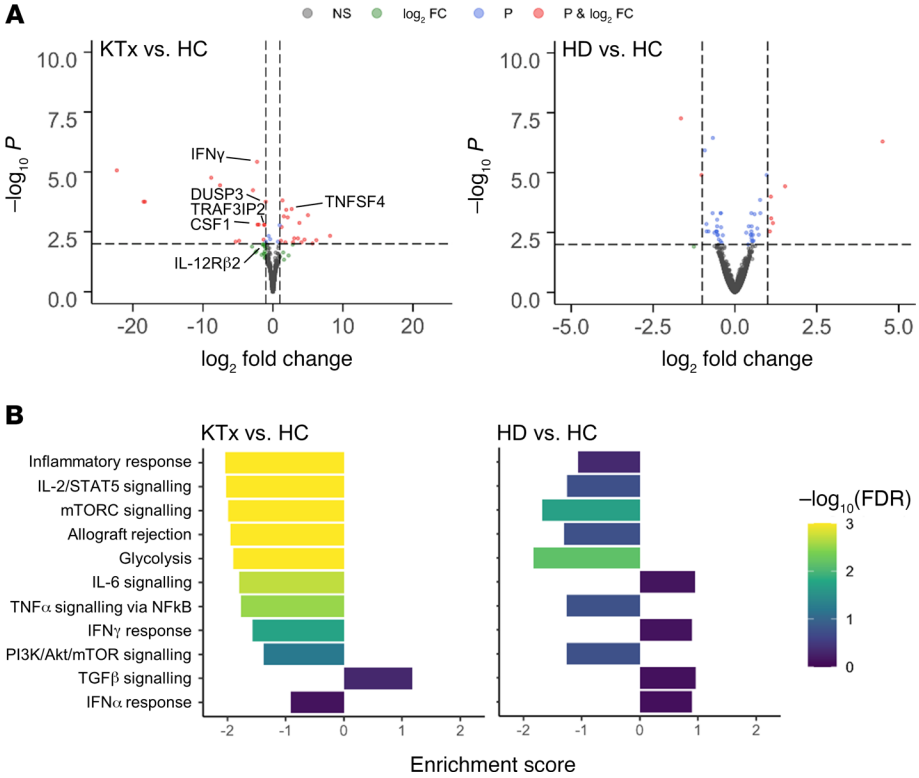

Figure 5. Analysis of differentially expressed genes in vaccine-specific Th cells. (**A**) Volcano plots depicting the $-\log_{10}$ FDR value and $\log_2$ fold changes of all expressed genes for comparisons of KTx patients vs. HCs (left) and HD patients vs. HCs (right). Thresholds for the FDR of 0.01 (*P*) and for the absolute $\log_2$ fold change of 1 are indicated by dotted lines; genes passing 0 (NS – not significant), 1, or both filters are color coded. Exemplary genes involved in cellular activation are annotated. (**B**) Enrichment scores and FDR values for different hallmark gene sets. Direction of the enrichment scores indicates up- or downregulation in the respective comparison. KTx, $n = 3$; HD, $n = 4$; HCs, $n = 4$.

Cell isolation and stimulation. Serum was collected and immediately cryopreserved. PBMCs were isolated from heparinized blood by Ficoll-Paque density gradient centrifugation and cryopreserved in liquid nitrogen. For antigen-specific T cell analysis, 3 to 5×10^6 PMBCs per stimulation were thawed and washed twice in prewarmed RPMI 1640 medium (containing 0.3 mg/ml glutamine, 100 U/ml penicillin, 0.1 mg/ml streptomycin, 20% FCS, and 25 U/ml benzonase; Santa Cruz Biotechnology Inc.), rested for 2 hours in culture medium (RPMI 1640 with glutamine, antibiotics, and 10% human AB serum, all Biochrom), and stimulated with SARS-CoV-2 spike or CEF peptide mix for 16 hours. Brefeldin A (10 μg/ml, Sigma-Aldrich) was added after 2 hours, enabling intracellular molecule retention. Due to cell number limitations, CEF stimulation was not conducted for all individuals. The same quantity of DMSO contained in peptide mixes was added to the unstimulated control samples.

Flow cytometric analysis. For detection of surface molecules, antibodies against CD3 (clone SK7, BioLegend), CD4 (clone SK3, BD), CD8 (clone SK1, eBioscience), CD45RO (clone UCHL1, BioLegend), CD62L (clone DREG-56, BioLegend), PD-1 (clone EH12.1, BD), and CD28 (clone CD28.2, BD) were used. Unwanted cells were excluded via a "dump channel" containing $CD14^+$ (clone M5E2, BioLegend), $CD19^+$ (clone HIB19, BioLegend), and dead cells (fixable live/dead, BioLegend). After stimulation, cells were fixed in FACS Lysing Solution (BD), permeabilized with FACS Perm II Solution (BD), and intracellularly stained with anti-CD154 (clone 24–31, BioLegend), anti-CD137 (clone 4B4-1, BioLegend), anti-CD69 (clone FN50, BioLegend), anti–TNF-α (clone MAb11, BioLegend), anti–IFN-γ (clone 4SB3, Ebioscience), anti–IL-2 (clone MQ1-17H12, BioLegend), anti-Ki67 (clone B56, BD), and anti–IL-4 (clone MP4-25D2, BioLegend). Cells were analyzed on a FACS Fortessa X20 (BD) flow cytometer.

Enrichment of spike-specific $CD4^+$ T cells, RNA-Seq and data analysis. For transcriptome analysis, 10^7 PBMCs were stimulated for 16 hours with SARS-CoV-2 spike glycoprotein peptide mix in the presence of anti-CD40 (1 μg/ml, clone HB14, Miltenyi Biotec), enabling CD154 surface retention on antigen-reactive cells (46). Thereafter, specific cells were surface stained with anti-CD154 PE (clone 24–31, BioLegend) and magnetically preenriched using anti-PE Nanobeads (BioLegend) over MACS LS columns (Miltenyi Biotec). Spike-specific $CD3^+CD4^+DUMP^-CD154^+CD69^+$ cells were further sorted in single-cell mode to greater than 95% purity into reaction buffer containing round-shaped PCR tube lids on a FACSAria Fusion Cell Sorter (BD) and spun down immediately. RNA extraction and cDNA library preparation were conducted with the SMART-Seq, version 4, Ultra Low Input RNA Kit (Takara). Sequencing was performed at the BIH Core Unit Genomics using an Illumina NextSeq 500 platform with 75 bp paired ends reads. RNA-Seq reads were trimmed using cutadapt 1.18, retaining reads at least 50 bp long and with at most 10% N content. Following adapter trimming, alignment to the GRCh38 reference genome obtained from ENSEMBL (47) was performed using STAR 2.7.1a (48),retaining only properly paired, uniquely mapping reads. Count matrices were generated using featureCounts from subread 2.0.1 (49) with annotation version GRCh38.98 obtained from ENSEMBL. Downstream processing was performed using DESeq2 1.22.2 (50) in R 3.5.1. Fold changes were shrunk using the ashr method (51). Annotations were added using biomaRt 2.38.0 (52). Differentially regulated pathways between groups were determined by Gene Set Enrichment Analysis (GSEA 4.1.0; ref. 53) using the hallmark gene set database (54). In order to ensure participant confidentiality, raw data will be available under controlled access in the European Genome-Phenome Archive repository (EGAS00001005280).

FACS data analysis. FACS data were analyzed with FlowJo, version 10 (BD). The gating strategy for analysis of antigen-specific T cells is depicted in Supplemental Figure 1A. A T cell response was considered positive when peptide mix–stimulated cultures contained at least 2-fold higher frequencies of $CD154^+CD137^+$ (for $CD4^+$ T cells) or $CD137^+$IFN-γ^+ (for $CD8^+$ T cells) cells as compared with the unstimulated control (SI of 2) with at least 20 events; given these prerequisites, no further background substraction was applied. Coexpression of cytokines was analyzed via Boolean gating. Unsupervised analysis

was conducted using tSNE included in Cytobank (Beckman Coulter). For that, data sets from spike-specific responders were pregated in FlowJo on CD154$^+$CD137$^+$ CD4$^+$ cells, followed by concatenation for each group and import into Cytobank.

Statistics. Statistical examination and composition of ELISA and FACS data–derived graphs were executed using GraphPad Prism, version 8. Parameter distribution was assessed using the Kolmogorov-Smirnov test. Depending on normal distribution, ANOVA (with Holm-Šidák′s post hoc test) or Kruskal-Wallis test (with Dunn's post hoc test) were chosen for multiple comparisons. For 2-group comparisons, 2-tailed, unpaired *t* test or Mann-Whitney *U* test was used. The relationship between 2 variables was examined by simple linear regression analysis. For analysis of contingency tables, Fisher's exact test was applied. In all tests, a value of $P < 0.05$ was considered significant.

Study approval. The study protocol was approved by the ethics committees of the Charité-Universitätsmedizin Berlin (EA4/188/20), Universitätsmedizin Greifswald, Greifswald, Germany (BB 019/21), and Sachsen-Anhalt, Germany (EA7/21) and carried out in compliance with their guidelines. All participants gave written, informed consent in accordance with the Declaration of Helsinki.

Author contributions

AS designed the study, performed research, analyzed data, and wrote the manuscript. E Schrezenmeier, UAW, AP, FB, and KB designed the study and analyzed data. HSH analyzed data. E Storz, VP, YB, CT, and OH performed research. LMLT, SL, DS, NL, HS, BJ, TZ, and KJ performed research and analyzed data. CC and AD designed the study. MC, FH, and KK designed the study and wrote the manuscript.

Acknowledgments

The authors are grateful to Michael Moesenthin and Peter Bartsch (Dialysezentrum Burg); Ralf Kühn and Dennis Heutling (Dialyse Tangermünde); Petra Pfand-Neumann (MVZ Diaverum Neubrandenburg); and Jörg-Detlev Lippert (Nierenzentrum Köthen) for patient recruitment. We further thank the Charité Universitätsmedizin Benjamin Franklin Flow Cytometry Core Facility (M. Fernandes and A. Branco), which is supported by DFG Instrument grants (INST 335/597-1 FUGG, INST 335/777-1 FUGG). The study was supported by a grant from the Sonnenfeldstiftung (Berlin, Germany) to Arne Sattler and Katja Kotsch; DFG grants (KO 2270/7-1, KO-2270/4-1) to Katja Kotsch; and project funding from Chiesi GmbH to Arne Sattler, Katja Kotsch, and Fabian Halleck. E Schrezenmeier is a participant in the BIH-Charité Clinician Scientist Program funded by the Charité-Universitätsmedizin Berlin and the BIH and received further support (BCOVIT, 01KI20161) from the Federal Ministry of Education and Research (BMBF). OH was supported by the Heidelberg Bioscience International Graduate School MD/PhD program (Heidelberg University, Germany). HS received funding from the Ministry for Science, Research and Arts of Baden-Württemberg, Germany, and the European Commission (HORIZON2020 Project SUPPORT-E, no. 101015756). SL was supported by a BMBF grant (01ZZ2001).

Address correspondence to: Arne Sattler or Katja Kotsch, Department for General and Visceral Surgery, Charité-Universitätsmedizin Berlin, Hindenburgdamm 30, 12203 Berlin, German. Phone: 49.30.450552427; Email: arne.sattler@charite.de (AS); Email: katja.kotsch@charite.de (KK).

1. Kato S, et al. Aspects of immune dysfunction in end-stage renal disease. *Clin J Am Soc Nephrol*. 2008;3(5):1526–1533.
2. Blazquez-Navarro A, et al. BKV, CMV, and EBV interactions and their effect on graft function one year post-renal transplantation: results from a large multi-centre study. *EBioMedicine*. 2018;34:113–121.
3. Ravanan R, et al. SARS-CoV-2 infection and early mortality of waitlisted and solid organ transplant recipients in England: A national cohort study. *Am J Transplant*. 2020;20(11):3008–3018.
4. Ng JH, et al. Outcomes of patients with end-stage kidney disease hospitalized with COVID-19. *Kidney Int*. 2020;98(6):1530–1539.
5. Jager KJ, et al. Results from the ERA-EDTA Registry indicate a high mortality due to COVID-19 in dialysis patients and kidney transplant recipients across Europe. *Kidney Int*. 2020;98(6):1540–1548.
6. Kates OS, et al. COVID-19 in solid organ transplant: A multi-center cohort study [published online August 7, 2020]. *Clin Infect Dis*. https://doi.org/10.1093/cid/ciaa1097.
7. Polack FP, et al. Safety and efficacy of the BNT162b2 mRNA Covid-19 vaccine. *N Engl J Med*. 2020;383(27):2603–2615.
8. Baden LR, et al. Efficacy and safety of the mRNA-1273 SARS-CoV-2 vaccine. *N Engl J Med*. 2021;384(5):403–416.
9. Sahin U, et al. BNT162b2 induces SARS-CoV-2-neutralising antibodies and T cells in humans [preprint]. https://doi.org/10.1101/2020.12.09.202451 75. Posted on medRxiv December 11, 2020.
10. Dagan N, et al. BNT162b2 mRNA Covid-19 vaccine in a nationwide mass vaccination setting. *N Engl J Med*. 2021;384(15):1412–1423.
11. Broeders NE, et al. Influenza A/H1N1 vaccine in patients treated by kidney transplant or dialysis: a cohort study. *Clin J Am Soc Nephrol*. 2011;6(11):2573–2578.
12. Brakemeier S, et al. Immune response to an adjuvanted influenza A H1N1 vaccine (Pandemrix(®)) in renal transplant recipients. *Nephrol Dial Transplant*. 2012;27(1):423–428.
13. Friedrich P, et al. Comparing humoral and cellular immune response against HBV vaccine in kidney transplant patients. *Am J Transplant*. 2015;15(12):3157–3165.
14. Elhanan E, et al. A randomized, controlled clinical trial to evaluate the immunogenicity of a PreS/S hepatitis B vaccine Sci-B-Vac, as compared to Engerix B((R)), among vaccine naive and vaccine non-responder dialysis patients. *Clin Exp Nephrol*. 2018;22(1):151–158.
15. Cowan M, et al. Impact of immunosuppression on recall immune responses to influenza vaccination in stable renal transplant recipients. *Transplantation*. 2014;97(8):846–853.
16. Betts MR, et al. Analysis of total human immunodeficiency virus (HIV)-specific CD4(+) and CD8(+) T-cell responses: relationship to viral load in untreated HIV infection. *J Virol*. 2001;75(24):11983–11991.
17. Sattler A, et al. SARS-CoV-2-specific T cell responses and correlations with COVID-19 patient predisposition. *J Clin Invest*. 2020;130(12):6477–6489.
18. Shabir S, et al. Cytomegalovirus-associated CD4(+) CD28(null) cells in NKG2D-dependent glomerular endothelial injury and kidney allograft dysfunction. *Am J Transplant*. 2016;16(4):1113–1128.
19. Kim C, et al. The life cycle of a T cell after vaccination - where does immune ageing strike? *Clin Exp Immunol*. 2017;187(1):71–81.
20. Litjens NH, et al. Impaired immune responses and antigen-specific memory CD4+ T cells in hemodialysis patients. *J Am Soc Nephrol*. 2008;19(8):1483–1490.
21. Boyarsky BJ, et al. Antibody response to 2-dose SARS-CoV-2 mRNA vaccine series in solid organ transplant recipients. *JAMA*. 2021;325(21):2204–2206.
22. Eickenberg S, et al. Mycophenolic acid counteracts B cell proliferation and plasmablast formation in patients with systemic lupus erythematosus. *Arthritis Res Ther*. 2012;14(3):R110.
23. Deepak P, et al. Glucocorticoids and B cell depleting agents substantially impair immunogenicity of mRNA vaccines to SARS-CoV-2 [preprint]. https://doi.org/10.1101/2021.04.05.21254656. Posted on medRxiv April 9, 2021.
24. McMahan K, et al. Correlates of protection against SARS-CoV-2 in rhesus macaques. *Nature*. 2021;590(7847):630–634.

25. Tan AT, et al. Early induction of functional SARS-CoV-2-specific T cells associates with rapid viral clearance and mild disease in COVID-19 patients. *Cell Rep*. 2021;34(6):108728.
26. Van Braeckel E, et al. Polyfunctional CD4(+) T cell responses in HIV-1-infected viral controllers compared with those in healthy recipients of an adjuvanted polyprotein HIV-1 vaccine. *Vaccine*. 2013;31(36):3739–3746.
27. Savic M, et al. Distinct T and NK cell populations may serve as immune correlates of protection against symptomatic pandemic influenza A(H1N1) virus infection during pregnancy. *PLoS One*. 2017;12(11):e0188055.
28. Lindenstrom T, et al. Tuberculosis subunit vaccination provides long-term protective immunity characterized by multifunctional CD4 memory T cells. *J Immunol*. 2009;182(12):8047–8055.
29. Sekine T, et al. Robust T cell immunity in convalescent individuals with asymptomatic or mild COVID-19. *Cell*. 2020;183(1):158–168.
30. Stervbo U, et al. Age dependent differences in the kinetics of γδ T cells after influenza vaccination. *PLoS One*. 2017;12(7):e0181161.
31. Rea IM, et al. Age and age-related diseases: role of inflammation triggers and cytokines. *Front Immunol*. 2018;9:586.
32. Pangrazzi L, et al. "Inflamm-aging" influences immune cell survival factors in human bone marrow. *Eur J Immunol*. 2017;47(3):481–492.
33. Bouvy AP, et al. T cells exhibit reduced signal transducer and activator of transcription 5 phosphorylation and upregulated coinhibitory molecule expression after kidney transplantation. *Transplantation*. 2015;99(9):1995–2003.
34. Brabletz T, et al. Transforming growth factor beta and cyclosporin A inhibit the inducible activity of the interleukin-2 gene in T cells through a noncanonical octamer-binding site. *Mol Cell Biol*. 1993;13(2):1155–1162.
35. Mendel I, Shevach EM. Activated T cells express the OX40 ligand: requirements for induction and costimulatory function. *Immunology*. 2006;117(2):196–204.
36. Vafadari R, et al. Tacrolimus inhibits NF-κB activation in peripheral human T cells. *PLoS One*. 2013;8(4):e60784.
37. Vaeth M, et al. Store-operated Ca(2+) entry controls clonal expansion of t cells through metabolic reprogramming. *Immunity*. 2017;47(4):664–679.
38. L'Huillier AG, et al. T-cell responses following natural influenza infection or vaccination in solid organ transplant recipients. *Sci Rep*. 2020;10(1):10104.
39. Tsuda K, et al. Calcineurin inhibitors suppress cytokine production from memory T cells and differentiation of naïve T cells into cytokine-producing mature T cells. *PLoS One*. 2012;7(2):e31465.
40. Ahrends T, et al. $CD4^+$ T cell help creates memory $CD8^+$ T cells with innate and help-independent recall capacities. *Nat Commun*. 2019;10(1):5531.
41. Ahrends T, et al. $CD4^+$ T cell help confers a cytotoxic T cell effector program including coinhibitory receptor downregulation and increased tissue invasiveness. *Immunity*. 2017;47(5):848–861.
42. Lai YP, et al. CD4+ T cell-derived IL-2 signals during early priming advances primary CD8+ T cell responses. *PLoS One*. 2009;4(11):e7766.
43. Schrezenmeier E, et al. Immunogenicity of COVID-19 tozinameran vaccination in patients on chronic dialysis [preprint]. https://doi.org/10.1101/2021.03.31.21254683. Posted on medRxiv April 6, 2021.
44. Rambal V, et al. Differential influenza H1N1-specific humoral and cellular response kinetics in kidney transplant patients. *Med Microbiol Immunol*. 2014;203(1):35–45.
45. Jahrsdorfer B, et al. Characterization of the SARS-CoV-2 neutralization potential of COVID-19-convalescent donors. *J Immunol*. 2021;206(11):2614–2622.
46. Frentsch M, et al. Direct access to CD4+ T cells specific for defined antigens according to CD154 expression. *Nat Med*. 2005;11(10):1118–1124.
47. Yates AD, et al. Ensembl 2020. *Nucleic Acids Res*. 2020;48(D1):D682–D688.
48. Dobin A, et al. STAR: ultrafast universal RNA-seq aligner. *Bioinformatics*. 2013;29(1):15–21.
49. Liao Y, et al. featureCounts: an efficient general purpose program for assigning sequence reads to genomic features. *Bioinformatics*. 2014;30(7):923–930.
50. Love MI, et al. Moderated estimation of fold change and dispersion for RNA-seq data with DESeq2. *Genome Biol*. 2014;15(12):550.
51. Stephens M. False discovery rates: a new deal. *Biostatistics*. 2017;18(2):275–294.
52. Durinck S, et al. Mapping identifiers for the integration of genomic datasets with the R/Bioconductor package biomaRt. *Nat Protoc*. 2009;4(8):1184–1191.
53. Subramanian A, et al. Gene set enrichment analysis: a knowledge-based approach for interpreting genome-wide expression profiles. *Proc Natl Acad Sci U S A*. 2005;102(43):15545–15550.
54. Liberzon A, et al. Molecular signatures database (MSigDB) 3.0. *Bioinformatics*. 2011;27(12):1739–1740.